Material and methods

Protein expression and purification.

Osh6p was cloned in pGEX-4T-3 vector to code for GST-fused constructs (gift from W. Prinz). The different site-specific mutations or deletion in Osh6p were obtained by the Quikchange kit (Agilent). For the truncated Δ69-Osh6p mutant, a short GGGG linker was introduced between the protein and GST to facilitate the cleavage by thrombin. The C2 domain of lactadherin (*Bos. Taurus*, obtained by AddGene, residue 270-427) was cloned in a pGEX-4T-3 vector. The $C2_{Lact}$ sequence was then mutated to replace two solvent-accessible cysteines (C270, C427) by alanine and to introduce a cysteine into a region near the putative PS-binding site (H352C mutation). All the mutations or deletions were checked by DNA sequencing.

GST-Osh4p, GST-Osh6p and mutants were expressed in *E. coli* at 30°C overnight whereas the GST-PH_{FAPP} and GST-$C2_{Lact}$ were expressed at 37°C for 3 h upon induction with 1 mM IPTG (at OD_{600}= 0.6). All purification steps were conducted in 50 mM Tris, pH 7.4, 120 mM NaCl, 2 mM DTT, supplemented during the first purification steps with PMSF (1 mM), bestatine (1 μM), pepstatine (10 μM), phosphoramidon (10 μM) and protease inhibitor tablets (Roche). Cells were lysed by a French press and the lysate was centrifuged at 200,000 g for 1 hour. The supernatant was applied to Glutathione Sepharose 4B beads. After 3 washing steps, the beads were incubated with thrombin at 4°C overnight to cleave the GST fusion and allow the release of proteins. All constructs contain an N-terminal GS sequence from the thrombin cleavage site. All constructs were next purified by gel filtration on a Sephacryl S300 HR XK16-70 column.

For NBD labeling of PH_{FAPP} or $C2_{Lact,}$ the crude eluate was mixed (after DTT removal by gel filtration on illustra NAP-10 columns (GE Healthcare)) with a 10-fold excess of N,N'-dimethyl-N-(iodoacetyl)-N'-(7-nitrobenz-2-oxa-1,3-diazol-4-yl)ethylenediamine (IANBD-amide, Molecular Probes). After 90 min on ice, the reaction was stopped by adding a 10-fold excess of L-cysteine over the probe. The free probe was removed by gel filtration on a Sephacryl S200 HR XK16-70 column. The labeled protein was analyzed by SDS-PAGE and UV-visible spectroscopy. The gel was directly visualized in a fluorescence imaging system (FUJI LAS-3000 fluorescence imaging system) to detect NBD-labeled protein excited in near-UV and then stained with Sypro Orange to determine the purity of NBD-labeled protein. The labeling yield (≈ 100 %) was estimated from the ratio of the optical density (OD) of tyrosine and tryptophan at 280 nm (ε=29,450 $M^{-1}.cm^{-1}$ for PH_{FAPP}, ε=45,045 $M^{-1}.cm^{-1}$ for $C2_{Lact,}$) and NBD at 495 nm (ε=25,000 $M^{-1}.cm^{-1}$). For all purified proteins, the concentration was determined by a BCA assay, by SDS-PAGE analysis using a BSA standard curve and UV spectrometry.

Preparation of liposomes

DOPC (1,2-dioleoyl-*sn*-glycero-3-phosphocholine), DOPS (1,2-dioleoyl-*sn*-glycero-3-phosphoserine) , POPS (1-palmitoyl-2-oleoyl-*sn*-glycero-3-phosphoserine) , DPPS (1,2-dipalmitoyl-*sn*-glycero-3-phosphoserine), brain PI4P (L-α-phosphatidylinositol-4-phosphate), DNS-PE (1,2-dioleoyl-*sn*-glycero-3-phosphoethanolamine-N-(5-dimethylamino-1-naphthalenesulfonyl)), NBD-PE (1,2-dioleoyl-*sn*-glycero-3-phosphoethanolamine-N-(7-nitro-2-1,3-benzoxadiazol-4-yl)), Rhod-PE (1,2-dipalmitoyl-*sn*-glycero-3-phosphoethanolamine-N-(lissamine rhodamine B

sulfonyl)) were purchased from Avanti Polar Lipids. 16:0/16:0-PI4P (1,2-dipalmitoyl-*sn*-glycero-3-phosphoinositol-4-phosphate) was from Echelon Lipids Inc. and dehydroergosterol (DHE) was from Sigma Aldrich. The concentration of DHE in stock solution in MeOH was determined by UV-spectroscopy using an extinction coefficient of 13,000 $M^{-1}.cm^{-1}$.

Lipids in stock solutions in $CHCl_3$ were mixed at the desired molar ratio. The solvent was removed in a rotary evaporator. For lipid films including PI4P the mix was pre-warmed to 33°C for 5 minutes prior to drying under vacuum. The films were then hydrated in 50 mM Hepes, pH 7.2, 120 mM K-acetate (HK buffer) to obtain a suspension of multilamellar liposomes. After five thawing-freezing cycles, the suspensions were extruded through polycarbonate filters of 0.2 µm pore size using a mini-extruder (Avanti Polar Lipids). Liposomes were stored at 4°C and in the dark when containing fluorescent lipids and used within 2 days.

Fluorimetric activity assays.

Most of the fluorimetric activity assays were carried out in a Shimadzu RF 5301-PC fluorimeter. The sample (volume 600 µL) was placed in a cylindrical quartz cell, continuously stirred with a small magnetic bar and thermostated at 30°C. At the indicated time, sample was injected from stock solutions with Hamilton syringes through a guide in the cover of the fluorimeter. Binding measurement of NBD-$C2_{Lact}$ with liposomes was performed with a Tecan Infinite M1000.

PI4P extraction assay

The sample (150µL) containing DOPC liposomes (150µM total lipids), doped with 4 % PI4P (3µM accessible) were mixed with NBD-PH_{FAPP} (250 nM) at 30 °C in a small quartz cuvette. PS or DHE were incorporated in liposome at the expense of DOPC. The NBD spectrum was recorded from 505 to 650 nm (bandwidth 5 nm) upon excitation at 490 nm (bandwidth 5 nm) before and 5 minutes after the injection of 3 µM Osh proteins. The intensity at 530 nm measured before and after the addition of protein corresponds to F_{max} and F. A control signal (F_o) was measured with the NBD-PH_{FAPP} (250 nM) in buffer or in the presence of liposome with the same composition but devoid of PI4P. The contribution of buffer or liposome alone was subtracted from the NBD signal. The percentage of PI4P extraction is given by $100*(1-((F-F_0)/(F_{max}-F_0)))$.

PS transport assay

A suspension (570 µL) of L_A liposome (200 µM total lipids) containing 2 % Rhod-PE and 5 % PS was incubated with 250 nM NBD-$C2_{Lact}$ at 30°C in HKM (HK + 1mM $MgCl_2$) buffer under constant stirring. The volume concentration of accessible PS (in the outer leaflet) is 5 µM. After 1 min, 30 µL of L_B liposome (200 µM total lipids, final concentration) were injected. After additional 3 min, Osh protein (200 nM) was injected. PS transport was followed by measuring the NBD signal at 530 nm (bandwidth 10 nm) upon excitation at 460 nm (bandwidth 1.5 nm). The NBD signal mirrors the distribution of NBD-$C2_{Lact}$ between L_A and L_B liposome. The amount of PS transported by Osh protein is determined by normalizing the NBD signal. To do so, we measured the NBD signal (F_{eq}) that corresponds to a situation where PS is fully equilibrated between liposomes. NBD-$C2_{Lact}$ (250 nM) was mixed with L_A and L_B liposome (200 µM total

lipid each) with a lipid composition similar to that of the liposomes used in the transport assay, except that each contains initially 2.5 % PS. The fraction of PS on L_A liposome, PS_A/PS_T, is directly equal to the fraction of $C2_{Lact}$ on L_A liposome and correspond to F_{Norm} $=0.5*(F-F_0/F_{eq}-F_0)$ with F_0 corresponding to the NBD signal prior to the addition of Osh protein. The amount of PS (in µM) transferred from L_A to L_B liposome corresponds to 5* F_{Norm}.

PI4P transport assay.

For the PI4P transport assay, a suspension (570 µL) of L_B liposome (200 µM total lipids) containing 2 % Rhod-PE and 4 % PI4P was incubated with 250 nM NBD-PH_{FAPP} at 30°C in HKM buffer under constant stirring. The volume concentration of accessible PI4P (in the outer leaflet) is 4 µM. After 1 min, 30 µL of L_A liposome (200 µM total lipids, final concentration) were injected. After additional 3 min, Osh protein (200 nM) was injected. The NBD signal is measured with the same set-up as for PS transport assay; the NBD signal mirrors the redistribution of NBD-PH_{FAPP} between L_A and L_B liposomes and was normalized to determinate the amount of PI4P transported by Osh protein. For this, we measured the NBD signal (F_{eq}) that corresponds to a situation where PI4P is fully equilibrated between liposomes. NBD-PH_{FAPP} (250 nM) was mixed with L_A and L_B liposome (200 µM total lipid each) that each contains initially 2 % PI4P. The fraction of PI4P on the surface of L_B liposome, $PI4P_B/PI4P_T$, is directly equal to the fraction of PH_{FAPP} on L_B liposome and correspond to F_{Norm} $=0.5*(F-F_0/F_{eq}-F_0)$ with F_0 corresponding to the NBD signal prior to the addition of Osh protein. The amount of PI4P (in µM) transferred from L_B to L_A liposomes corresponds to 4* F_{Norm}.

DHE extraction assay

The sample (150µL) containing DOPC liposomes (150 µM total lipids) doped with 2.5 % of DNS-PE and 2 % of DHE was incubated at 30 °C in a small quartz cuvette. Lipid extraction was followed by recording the dansyl signal at 525 nm (bandwidth 10 nm) upon DHE excitation at 310 nm (bandwidth 1.5 nm) before and 5 min after the addition of 3 µM Osh protein. The signal corresponds to F_{max} and F, respectively; the intensity signal corresponding to the maximal DHE extraction (F_0), was determined with 2mM methyl-β-cyclodextrin. The percentage of DHE extraction is given by $100*(1-((F-F_0)/(F_{max}-F_0))$.

Flotation experiments.

The protocol has been described in detail *(28)*. Briefly, proteins (0.75 µM) were incubated with NBD-PE containing liposomes (750 µM total lipids) in 150 µL HKM buffer at room temperature for 5 min. The suspension was adjusted to 30% sucrose by mixing 100 µL of a 75% (w/v) sucrose solution in HKM buffer and overlaid with 200 µL HKM containing 25% (w/v) sucrose and 50 µL sucrose-free HKM. The sample was centrifuged at 240,000 g in a swing rotor (TLS 55) for 1 h. The bottom (250 µL), middle (150 µL) and top (100 µL fractions were collected. The bottom and top fractions were analyzed by SDS-PAGE using Sypro-Orange staining and a FUJI LAS-3000 fluorescence imaging system.

Yeast Strains, Plasmids and Manipulations

Yeast manipulations were performed using standard methods and growth conditions. Strain *cho1Δ osh6Δ osh7Δ* was a gift from AC. Gavin, created in the BY4741 background (MAT*a can1Δ::STE2pr-LEU2 lyp1Δ ura3Δ0 leu2Δ0 his3Δ1 met15Δ0 cho1Δ::KANMX osh6Δ::HYGMX osh7Δ::NATMX*) (*9*). Strains *sac1Δ* and the wild-type strain BY4742 were from the Euroscarf collection (MAT*α* his3*Δ*1 leu2*Δ*0 lys2*Δ*0 ura3*Δ*0). The plasmid expressing Osh6p with a C-terminal mCherry tag *(*pRS315-*ADH1pr-OSH6-mCherry)* was a gift from AC. Gavin *(9)*, and the plasmid pRS416-LactC2-GFP was from Haematologic technologies. Mutagenesis of the pOsh6-mCherry plasmid to express the Osh6p single mutants L69D and K351E, double mutant H157A/H158A, and triple mutant H157A/H158A/K351E was performed using Quikchange site-directed mutagenesis (Agilent). The strain *sac1Δ cho1Δ osh6Δ osh7Δ* expressing $C2_{Lact}$-GFP and Osh6p-mCherry (ACY400) was generated by introducing a *sac1Δ::HIS3* disruption cassette into the strain *cho1Δ osh6Δ osh7Δ,* carrying the plasmids pLactC2-GFP and pOsh6-mCherry. The disruption was confirmed by PCR. To construct the *cho1Δ sac1-ts* strain, we first transformed the strain MFY62 (SEY6210.1 MATα *sac1Δ::TRP1* (*22*), gift from C. Stefan (MRC, UCL)) with a PCR-generated *cho1Δ::NAT* disruption cassette to generate ACY402. Deletion of *CHO1* was confirmed by PCR. In a second transformation step, plasmids carrying *sac1-23* ((*22*), plasmid pRS415 *sac1-23, CEN, LEU2*, gift from C. Stefan) and $C2_{Lact}$-GFP were introduced to generate strain ACY403 (SEY6210.1 *sac1Δ::TRP1* pRS415*sac1-23* pRS416-*LactC2-GFP).* The control strain ACY401 (SEY6210 *cho1Δ::NAT)* was constructed by introducing the *cho1Δ::NAT* disruption into the parental strain SEY6210 (MATa *ura3-52 leu2–3,112 his3Δ200 trp1-Δ901 lys2-801 suc2Δ9).*

Fluorescent Microscopy

Yeast strains were grown overnight at 30°C in appropriate SD medium to maintain plasmid selection. For strains carrying the *cho1Δ* mutation, SD medium was supplemented with 1 mM ethanolamine. Cells were harvested in mid-logarithmic phase (OD_{600}=0.6–0.8) and prepared for viewing on glass slides when assessing protein localization at steady state, or in a microfluidics chamber in the case of time-course experiments using lyso-PS (see below). When indicated, vacuolar staining was obtained by incubating cells with 100 μM CMAC (Life Technologies) for 10 min at 30°C, after which the cells were washed twice before viewing. Imaging was performed at room temperature, except in the case of the *sac1-ts* or *SAC1* control cells. Here, the cells were grown overnight at 26°C to mid-logarithmic phase and then either shifted to 38°C for the experiments at non-permissive temperature, or kept at 26°C.

The cellular localization of PS was monitored in *cho1Δ* strains after the addition of exogenous lyso-PS as was previously described *(9)*, with some modifications. 18:1 lyso-PS (1-oleoyl-2-hydroxy-*sn*-glycero-3-phospho-L-serine, Avanti Polar Lipids), which was stored in chloroform under argon, was dried under argon to remove the solvent and dissolved in SD medium to 54 μM. We used vortexing and heating to 37°C to improve the solubilization. The medium containing lyso-PS was always prepared fresh,

maintained at room temperature and used within a few hours after preparation. All lyso-PS containing solutions were kept in glass vials to minimize adsorption of lyso-PS.

For lyso-PS time course experiments, cells were injected into a YO4C microfluidics chamber using the Microfluidic Perfusion Platform (ONIX), driven by the interface software ONIX-FG-SW (CellASIC Corp.). Cells were trapped and maintained in a uniform focal plane. Normal growth conditions were maintained by flowing cells with SD medium or SD medium containing lyso-PS at 3 psi. The microfluidics device was coupled to a DMI6000 (Leica) microscope, equipped with an oil immersion plan apochromat 100x objective NA 1.4, a QuantEM cooled EMCCD camera (Photometrics), and a spinning-disk confocal system CSU22 (Yokogawa). GFP-tagged proteins, mCherry-tagged proteins and CMAC staining were visualized with a GFP Filter 535AF45, RFP Filter 590DF35, and DAPI Filter 450QM60, respectively. Images were acquired with MetaMorph 7 software (Molecular Devices). We always imaged cells in 5 z-sections separated by 0.5 µm, usually in four different fields of 512 x 512 pixels.

For the *sac1-ts* experiments, cells were incubated in batch in medium containing 54 µM lyso-PS for 40 min at the indicated temperature and imaged on the spinning disk system described above, with incubation chamber preheated to the same temperature. For the experiments at 38°C, cells were preincubated at this temperature for 60 min before the addition of lyso-PS.

Imaging of $C2_{Lact}$-GFP localization at steady state was performed with an LSM780 (Zeiss) confocal microscope system equipped with 488 and 561 excitation lasers (for GFP and mCherry, respectively), GaAsP spectral and PMT detectors, an oil immersion plan apochromat 63x objective NA 1.4, and ZEN software. Images were processed with ImageJ (NIH) and Photoshop (Adobe) for levels.

Quantification of $C2_{Lact}$-GFP localization in cells

Fluorescent images of $C2_{Lact}$-GFP were quantified using ImageJ (NIH) and the data was processed in Excel. We placed a line over each cell to obtain a 1D fluorescence intensity profile and we used the ImageJ plugin 'BAR: Find Peaks' to find the intensity values for the maxima and the minima in the profile. These values, along with the intensity values for each pixel were imported into Excel. We then calculated the average values for the two outer cellular intensity peaks ('peripheral peaks') and the two highest internal peaks ('internal peaks') and subtracted from these values the average value of intensity minima between the two peripheral peaks, to obtain the relative heights of intensity peaks. Finally, we normalized peak intensities by dividing the two relative peak values with average intensity of all pixels between the two peripheral peaks (*i.e.* average fluorescence within the cell, Figure S8A).

It is noteworthy that, in yeast, the ER can be seen surrounding the nucleus (perinuclear ER) as well as underneath the PM (cortical ER). At the resolution of light microscopy, cortical ER signal cannot be distinguished from PM signal. In the 1D intensity profiles, cytosolic localization of $C2_{Lact}$-GFP is represented by low peripheral and internal signal peaks. A concomitant increase in internal and peripheral signal peaks signifies ER localization, whereas a larger increase in peripheral compared to internal peaks signifies that $C2_{Lact}$-GFP localizes to the PM (see Figure S8A)

We quantified ~20 cells *per* experiment, in one z-section that was selected manually and that contained the strongest perinuclear fluorescent signal. To avoid bias in

our analysis, we selected cells at the beginning of the time course (when the $C2_{Lact}$-GFP signal is uniformly cytosolic) and followed the same cells throughout the time course. In the case of *sac1-ts* experiments, where we quantified $C2_{Lact}$-GFP localization after a batch incubation with lyso-PS, we selected a field of cells and quantified the signal in all cells in the selected field.

Crystal structure

Osh6p (1.3 $mg.mL^{-1}$) eluted from GST beads was incubated for 2 hours with DOPC liposomes containing 2 % brain PI4P and loaded with sucrose (2.75 mM total lipids). The sample (2 mL) was centrifuged at 400,000 × g for 20 min at 4°C in a fixed-angle rotor (TLA 100.1) to separate the protein loaded with PI4P from liposomes. The Osh6p:PI4P complex recovered in the supernatant was purified by gel filtration on a Sephacryl S200 HR XK16-50 column and concentrated at 3.1 $mg.mL^{-1}$. The Osh6p:PI4P complex was crystallized by hanging drop vapour diffusion method where 1 µL of protein sample in 20 mM Tris pH 8.0, 100 mM NaCl was mixed to 1 µL of reservoir solution containing 200 mM ammonium acetate, 100 mM Bis-tris pH 5.5 and 20 % PEG 3350 at 18°C. Native diffraction data from one crystal cryoprotected with 20 % (v/v) glycerol were collected to 2.55 Å resolution on the ID23-1 beamLine at the European Synchrotron Radiation Facilities (λ = 0. 97298 Å, 100K), Grenoble, France. Data were processed and scaled with XDS and XSCALE (*29*). The PI4P-bound Osh6p crystallized in the space group $P\ 2_1 2_1 2_1$ with cell parameters a = 114.11 Å, b = 122.26 Å, c = 141.49 Å, $\alpha = \beta = \gamma = 90°$, with four molecules *per* asymmetric unit. The X-ray structure was solved and refined using Phenix (phenix.automr, phenix.refine) (*30*) and COOT (*31*). Data collection and refinement statistics are summarized in Table S1. Figures were prepared with PyMOL (http://pymol.org/).

MD simulations

All simulations are based on the crystal structure of Osh6p bound to PS (PDB ID: 4B2Z) and to PI4P (PDB ID: 4PH7). All ionizable side chains, as well as the C- and N-termini were modeled in their default ionization state, with the exception of H157 and H158 residues that were modeled as positively charged in the PI(4)P simulations (*16*). The systems were immersed in a box of water of approximately 85x80x85 $Å^3$ containing approximately 17000 molecules. The box dimensions are chosen in such a way that the minimum distance between periodic images of the protein is always larger than 25 Å during the simulation. Neutrality of the system at physiological ion concentration (120 mM) was obtained by adding 41 (38) sodium and 38 (36) chloride ions to the aqueous phase in the case of PS (PI4P). The total number of atoms in our models is about 58000. After insertion of the protein, the system was minimized using a steepest descent algorithm and then heated up to 300K in 1200 ps while keeping positional restraints on crystallographic Cα atoms (Cαs) that were slowly removed in two successive runs of 3 ns at 300K. Positional restraints on crystallographic Cαs were set to 1000 kJ mol-1 nm-2 and 100 kJ mol-1 nm-2, respectively. The all-atom CHARMM27 (*32*) force field was used in combination with the TIP3P (*33*) model for water. The force field for PI4P was taken from (*16*). Electrostatic interactions were calculated with the Ewald particle mesh method (*34*) with a real space cutoff of 10 Å. Bonds involving hydrogen atoms were constrained using the LINCS algorithm (*35*) and the integration time step was set to 2 fs.

The system was coupled to a Bussi thermostat (*36*) and to an isotropic Parrinello-Rahman barostat (*36*) at a temperature of 300K and a pressure of 1 atm. The MD trajectories described in the text are the following: two MD runs of 1 μs each of Osh6p bound to 18:0/20:4-PI4P or 16:0/18:1-PS (POPS).

All data analysis was performed using GROMACS (*37)* utilities and all molecular images were made with Visual Molecular Dynamics (VMD) (*38*). All analyses reported are performed over the last 500 ns of the trajectories.

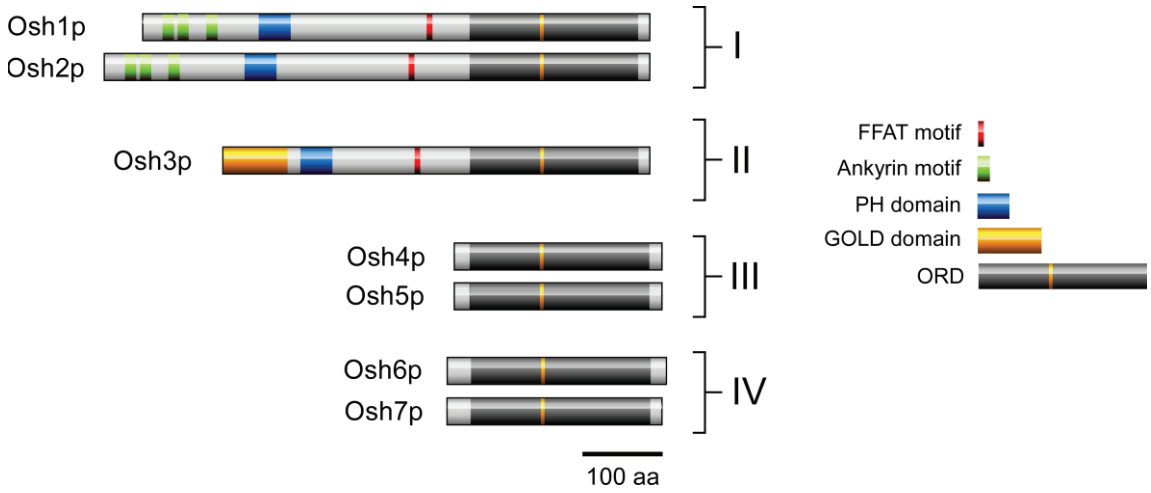

Figure S1. Description of the Osh proteins.
Osh proteins are classified into four different subclasses according to their sequence homology. FFAT: two phenylalanines in an acidic tract, GOLD : Golgi dynamics ; PH : Pleskstrin Homology ; ORD : oxysterol-related domain. Adapted from (*10*).

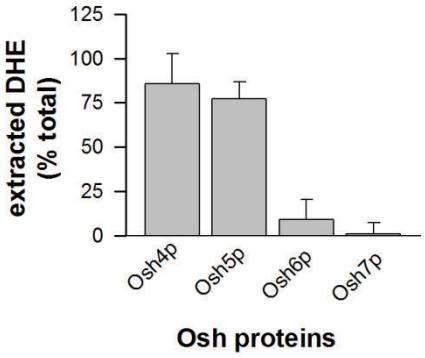

Figure S2. Osh6p and Osh7p do not extract DHE.
DHE extraction (2 %) from liposomes (150 μM, total lipids) was quantified by measuring the decrease in FRET between DHE and DNS-PE (2.5 %) 5 min after the addition of 3 μM Osh protein. Data were normalized in comparison to extraction of 10 mM methyl-β-cyclodextrin. Data are represented as a mean ± SEM (error bars, N=3)

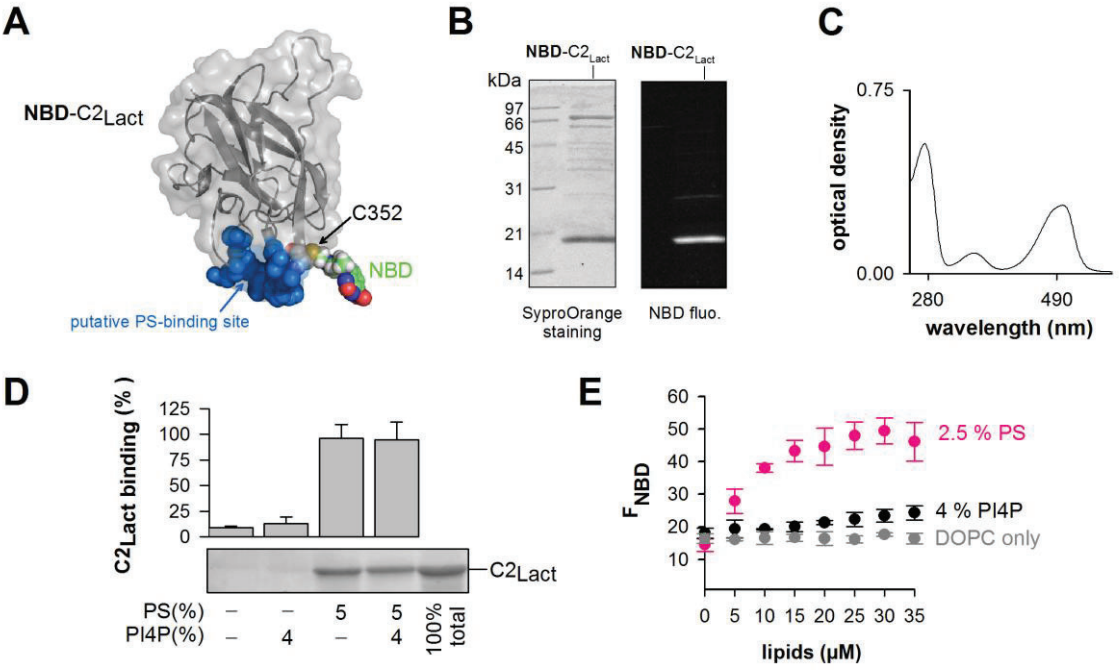

Figure S3. Characterization of the PS-sensor NBD-C2$_{Lact}$.
(A) Tridimensional model of the NBD-labeled C2$_{Lact}$ based on the crystal structure of the C2 domain of bovine Lactadherin (PDB entry: 3BN6 (*39*)). The solvent-exposed cysteines C240 and C427 are mutated for alanines whereas histidine H352 is replaced by a cysteine. An N,N'-dimethyl-N-(thioacetyl)-N'-(7-nitrobenz-2-oxa-1,3-diazol-4-yl)ethylenediamine moiety (in stick, with carbon in grey, nitrogen in blue and oxygen in red), built manually and energetically minimized, is grafted to the thiol function of C352, near the PS-binding site. The figure is prepared with PyMOL (http://pymol.org/). **(B)** SDS-PAGE of purified NBD-C2$_{Lact}$. The gel was directly visualized in a fluorescence imaging system to identify labeled proteins (right picture) and then stained with Sypro Orange to visualize all proteins and molecular weight markers (left picture) **(C)** UV-visible absorption spectrum of NBD-C2$_{Lact}$. Considering a purity grade of 100% for the protein, the optical density value at 280 nm (Trp) and 495 nm (IANBD) indicates that the C2 domain was labeled with the probe at a ~ 1:1 ratio. **(D)** Flotation assays show that C2$_{Lact}$ (1µM) in the presence of extruded 0.2 µm liposomes (1 mM total lipid) with different composition only binds to PS-containing liposomes. The incorporation of PI4P in liposome does not change the binding level. Value are represented as the mean ± SEM. (error bar, N=2). **(E)** Binding of NBD-C2$_{Lact}$ (250 nM) to liposomes of different composition (DOPC/POPS 97.5/2.5, DOPC/PI4P 96/4 or DOPC). The fluorescence measured at 535 nm (λ_{ex}=495 nm) was plotted as function of total lipid concentration. The increase in intensity indicates the interaction of the construct with liposomes. Data are represented as a mean ± SEM. (error bars, N=2-3).

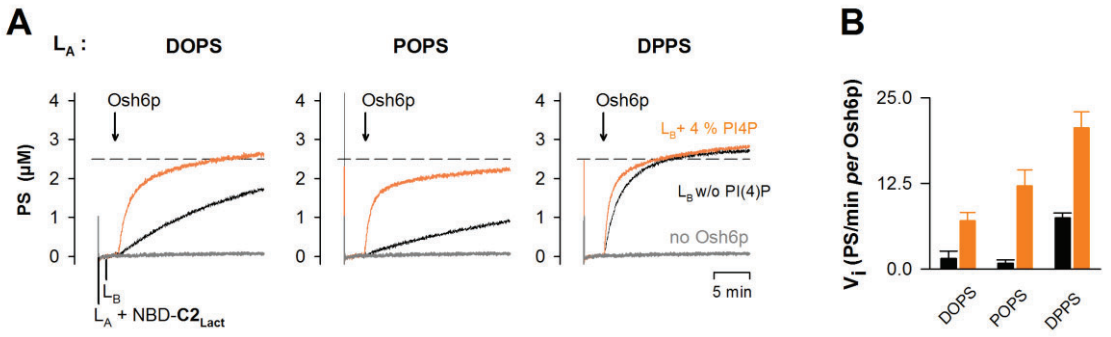

Figure S4. PS transport capacity of Osh6p is influenced by the length and saturation of PS molecules.

(**A**) DOPC liposomes (200 µM total lipids, L_A) containing 2 % Rhod-PE and 5 % 18:1/18:1-PS (DOPS), 16:0/18:1-PS (POPS) or 16:0/16:0-PS (DPPC) were mixed with NBD-$C2_{Lact}$ (250 nM) at 30°C. After one minute, DOPC liposomes (200 µM lipids, L_B) containing or not 4 % 16:0/16:0-PI4P were added. After 3 min, Osh6p (200 nM) was injected. The dashed line corresponds to full equilibration of PS between liposomes. (**B**) Initial rates of PS transport. Data are represented as a mean ± SEM (error bars, N=3)

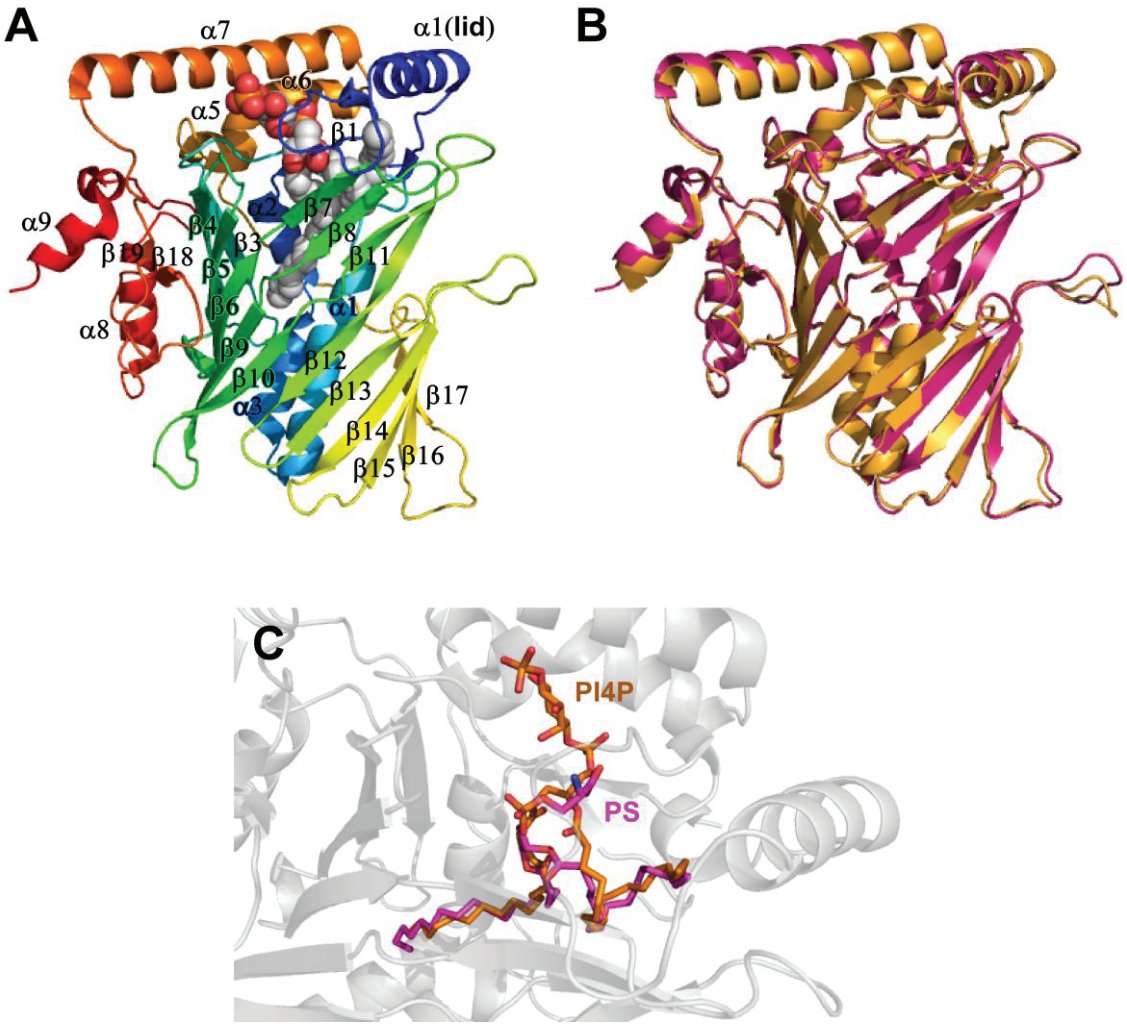

Figure S5. Structure of Osh6p in complex with PI4P.
(A) The overall structure of Osh6p-PI4P (PDB entry: 4PH7) is similar to that of Osh6p-PS (PDB entry: 4B2Z) (*9*) with a hydrophobic lipid-binding tunnel defined by an incomplete β-barrel (residues 133-317, in green) completed by a C-terminal region (residues 318-435, red-orange) and flanked by an N-terminal domain consisting in a two-stranded β-sheet and three α-helices (70-128, blue-green). PI4P is represented as sphere with carbon atoms colored in grey, oxygen atoms in red and phosphorus in orange. **(B)** Structure superposition of Osh6p in complex with 18:0/20:4-PI4P (in orange) or 16:0/18:1-PS (in pink). The lid (residues 35-69) adopts a similar conformation to shield the PI4P or PS molecule. **(C)** Superposition of 18:0/20:4-PI4P (colored in orange) and 16:0/18:1-PS (colored in pink) molecules in Osh6p. The backbone of the protein is shown in light-grey.

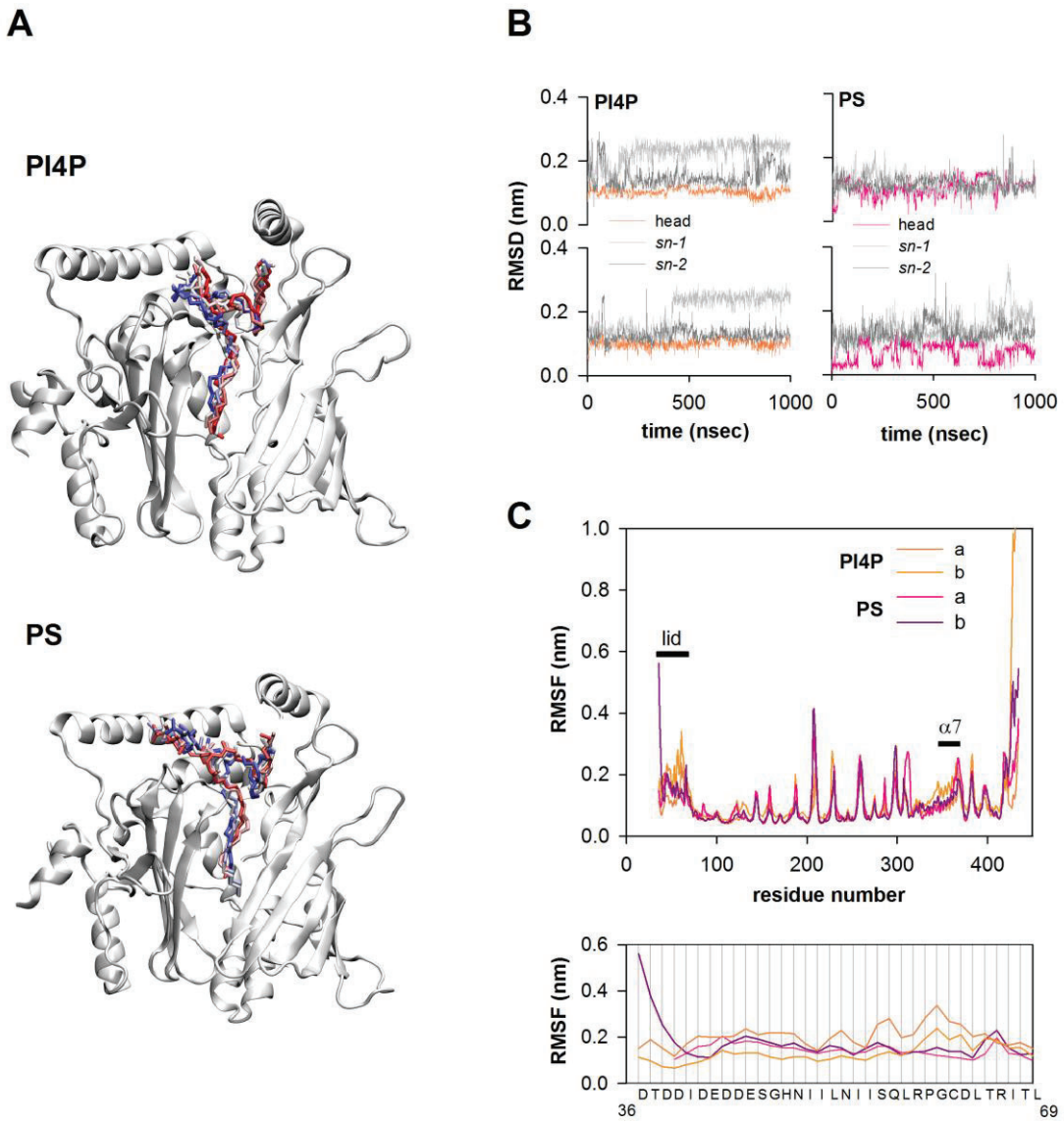

Figure S6. Molecular dynamic simulations of Osh6p in complex with PS or PI4P. **(A)** Dynamic of PI4P and PS inside the binding pocket of Osh6p. The time evolution of the lipids is shown during 1 µs of MD simulations with colors going from red (beginning of the MD trajectory) to blue (end of the trajectory). **(B)** Root-mean-square-deviation (RMSD) of PI4P or PS polar head and acyl chains determined for each case from two independent trajectories **(C)** Total root-mean-square positional fluctuations (RMSF) in Osh6p (residues 35-341), bound to 16:0/18:1-PS or 18:0/20:4-PI4P, indicative of the internal protein motion during 1 µs MD, determined for each case from two independent trajectories. The positions of the lid and α7 helix are indicated by black rectangles. *Lower insert :* RMSF of the 35-69 region (lid).

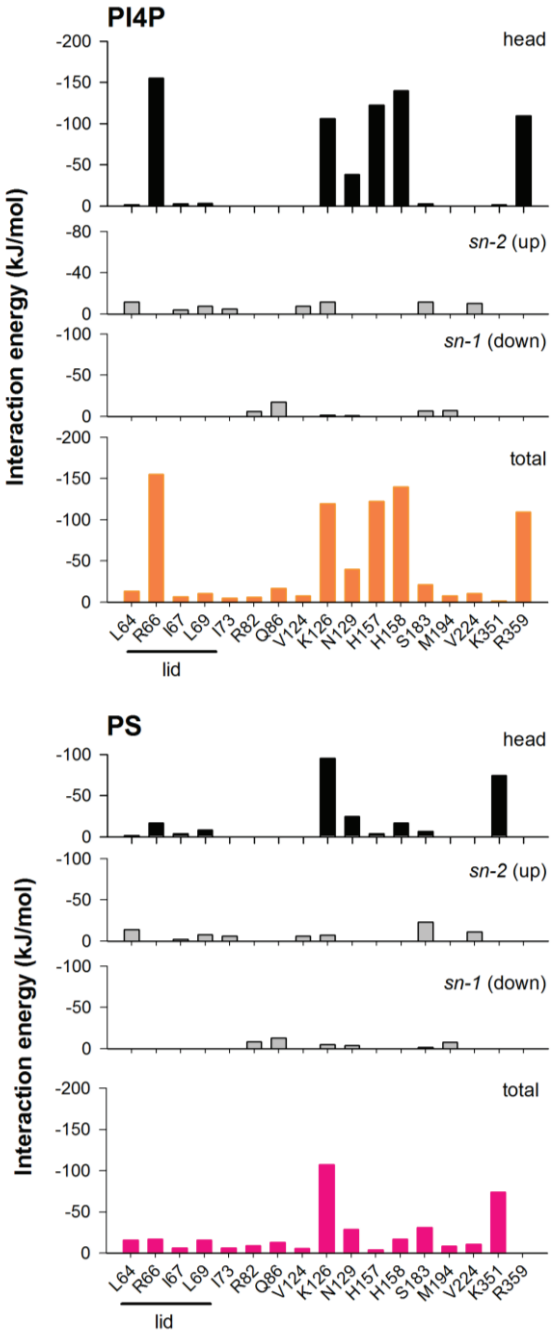

Figure S7. Interaction energy between Osh6p residues and 16:0/18:1-PS or 18:0/20:4-PI4P

Energy values are given for the residues that contribute the most to the binding of the two lipids to Osh6p. Interaction between residues and the whole lipid (PI4P: orange bar; PS : pink bar), the *sn-1* acyl-chain , *sn-2* acyl-chain (gray bar) or polar head of lipid (black bar). Data are represented as mean (N = 2).

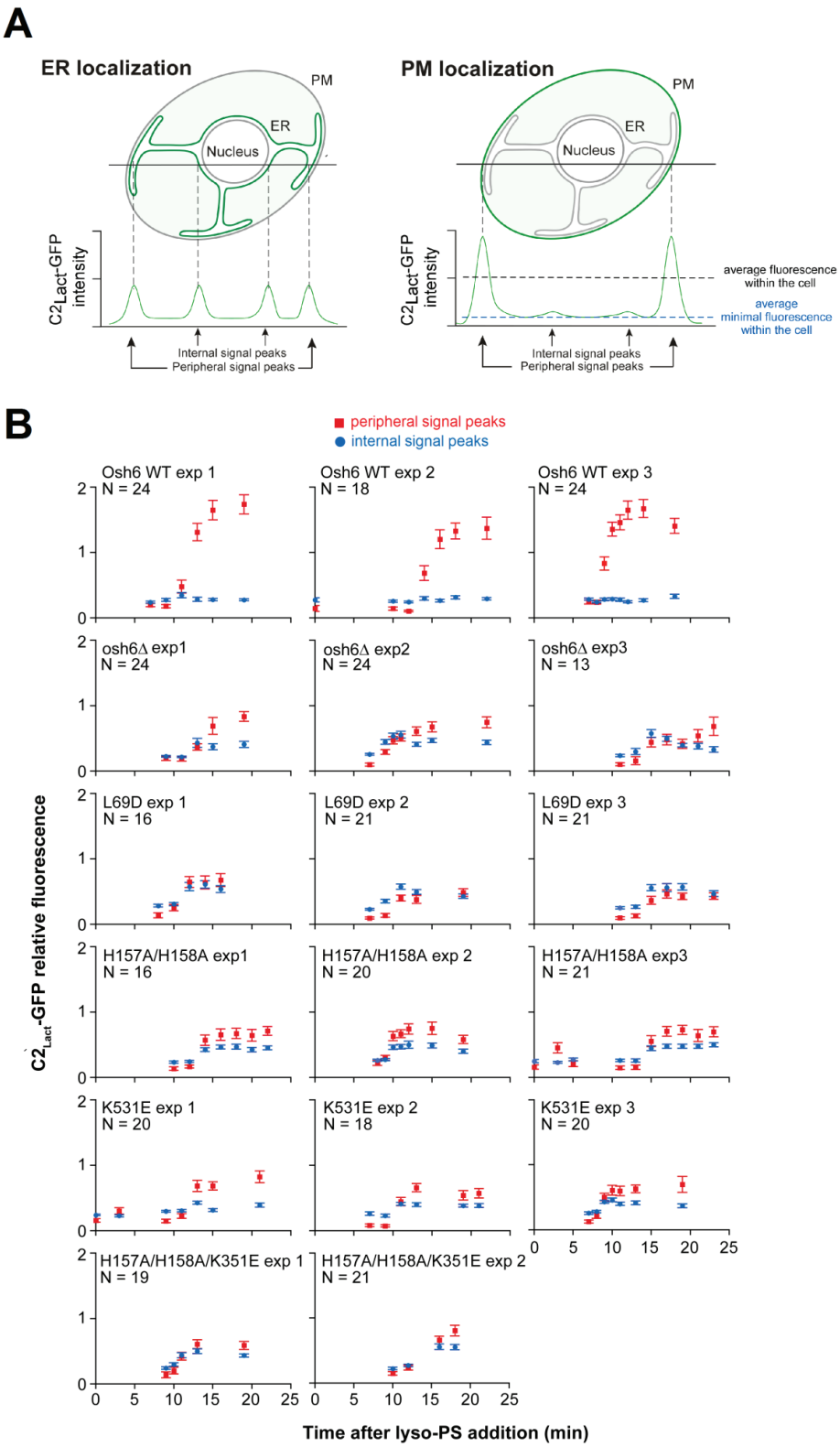

Figure S8. Quantification of the PS transport activity of Osh6p WT and mutants.
(see text next page)

(**A**) Schematic description of the 1D profile used to quantify $C2_{Lact}$-GFP localization (see details in Material and Method section) (**B**) Quantification of $C2_{Lact}$-GFP distribution showing relative fluorescence of peripheral and internal membrane intensity peaks for independent experiments. The same cells were analyzed at each time point. Data are represented as a mean ± SEM (error bars, N=number of cells). The graphs for each genotype presented in this figure (except for the triple mutant H157A/H158A/K351E) were combined to generate the plots in Fig.2F. Because of the variability of the length of the initial lag phase (before the ER-to-PM transport step mediated by Osh6p), the times were sometimes shifted in order to overlay the plots from individual experiments. The x-axis in Fig. 2F is therefore labeled 'time after signal transition', with time '0' representing the first time-point where we observe a transition from cytosolic to ER/PM localization of $C2_{Lact}$-GFP. In a few cases, some time-points from the 3 individual experiments could not be exactly matched; in such cases the average time of the individual time points was plotted and an x-error bar was added to the data point representing the time uncertainty at this data point. Our quantification procedure indicated that compared to an experiment in which yeast is devoid of Osh6p, no ER-to-PM transport of PS was seen after lyso-PS addition when Osh6p(L69D) was expressed. These data, along with our *in vitro* assays, confirmed previous observations (*9*), i.e. that Osh6p(L69D) is strongly deficient in transporting PS and can serve as negative control to which the other mutants can be directly compared.

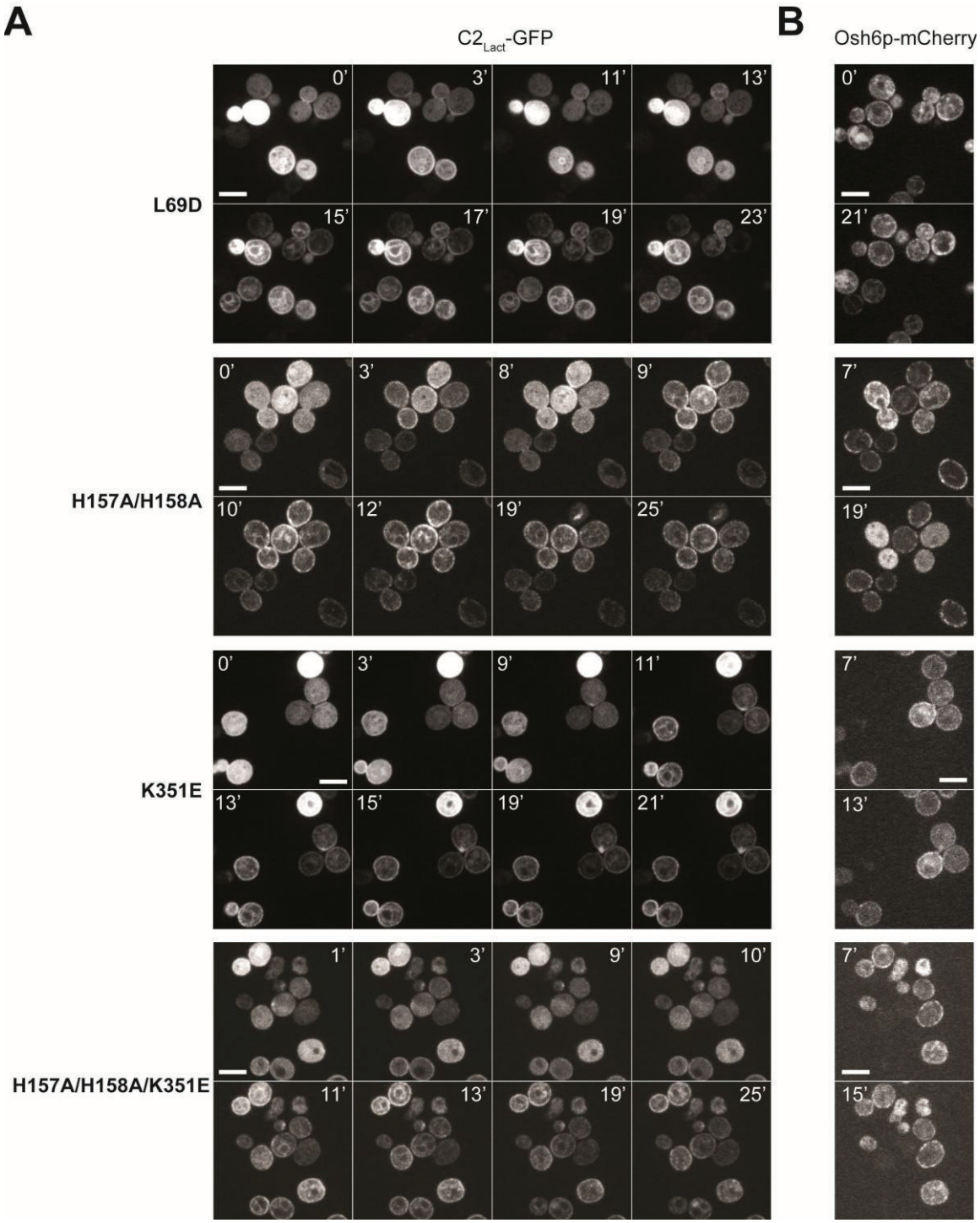

Figure S9. PS transport ability of Osh6p mutants
(see text next page)

(**A**) Detailed kinetic analysis of $C2_{Lact}$–GFP localization in *cho1Δosh6Δosh7Δ* cells (depleted for PS), expressing different mutants of Osh6p tagged with mCherry at the C-terminus, upon addition of 18:1 lyso-PS. Cells were maintained in a microfluidics chamber under a constant flow of cell medium, and medium containing lyso-PS was injected into the chamber at time 0. Images were taken every 2 min, or in some experiments every 1 min during the middle of the time-course; shown are the time-points when noticeable changes in the $C2_{Lact}$ signal occurred. The reported void volume of the microfluidics chamber at the flow rate used is ~3 min. At this time, a slight and transient increase in the $C2_{Lact}$ signal at the cell periphery was sometimes observed. Subsequently, $C2_{Lact}$-GFP returned to its initial cytosolic localization, until it began to relocalize to the ER membranes at ~12 min after lyso-PS addition (there is a variability of ± 3 min in this initial lag phase). (**B**) Localization of Osh6p mutants in the same time-course at two time-points, before and after the change in $C2_{Lact}$-GFP localization. All mutants were expressed at about the same level and could be observed at the cell cortex in some cells, whereas other cells displayed more cytosolic signal. Cells shown are representative of ~100 cells that were imaged in each experiment, and each experiment was repeated at least 3 times. Scale-bar: 5 μm

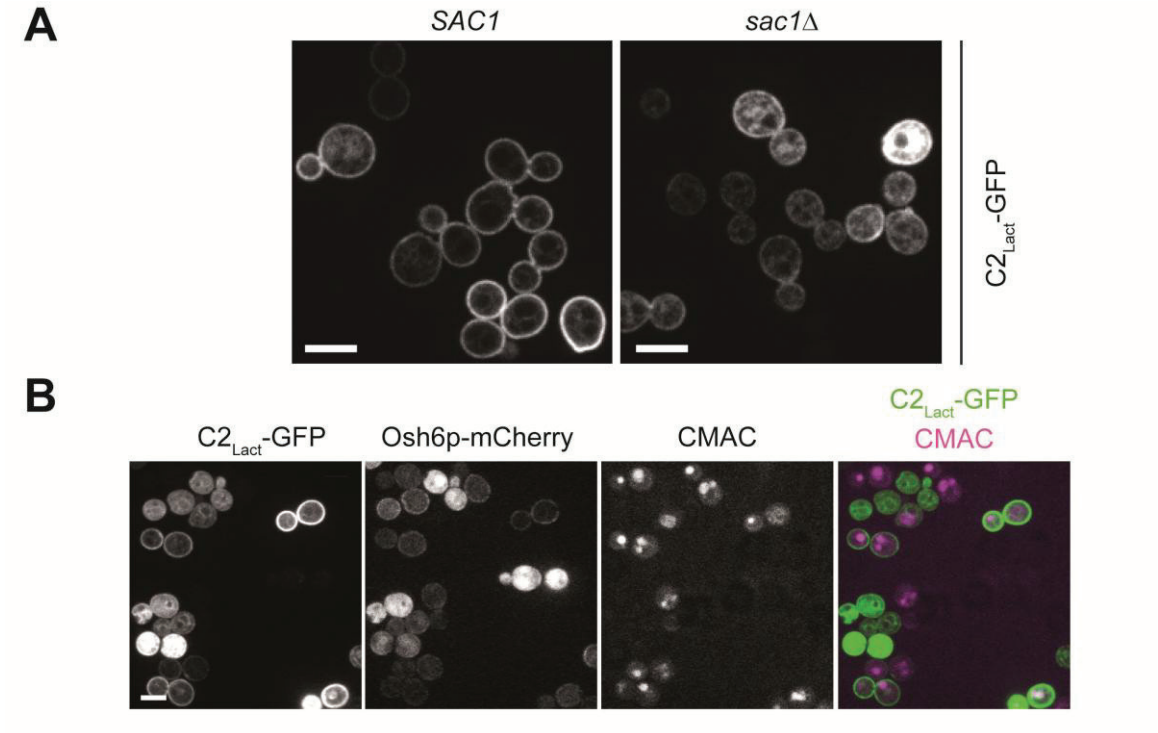

Figure S10. $C2_{Lact}$-GFP is mislocalized in cells lacking the PI4P phosphatase Sac1p. (**A**) Localization of the PS-reporter $C2_{Lact}$-GFP in *SAC1* (left panel) or *sac1Δ* cells (right panel) at steady state. (**B**) A larger field of cells from the same experiment as in Fig.3A at 19 min after lyso-PS addition, showing the localization of $C2_{Lact}$-GFP, Osh6-mCherry, the vacuolar dye CMAC (labeling only *SAC1* cells), and overlay of the green (GFP, in green) and blue (CMAC, in magenta) images. Note that Osh6p-mCherry is expressed in both *sac1Δ* and *SAC1* cells, but may be more cytosolic in cells lacking Sac1p. The genotypes of the two cell populations used in this experiment are *sac1Δcho1Δosh6Δ osh7Δ* p$C2_{Lact}$-GFP pOSH6-mCherry and *cho1Δosh6Δosh7Δ* p$C2_{Lact}$-GFP pOSH6-mCherry.

Table S1. Data collection and refinement statistics.

	Osh6p/PI4P PDB ID: 4PH7
Data collection	
Space group	$P\ 2_1 2_1 2_1$
Cell dimensions	
a, *b*, *c* (Å)	114.11, 122.26, 141.49
α, β, γ (°)	90.00, 90.00, 90.00
Resolution (Å)	48.56 – 2.55 (2.69 – 2.55)*
R_{sym}	0.106 (0.496)
$I / \sigma I$	15.65 (4.95)
Completeness (%)	100.00 (100.00)
Redundancy	8.2 (8.1)
Refinement	
Resolution (Å)	47.29 – 2.55
No. reflections	30,180
R_{work} / R_{free}	0.188 / 0.237
No. atoms	
protein	12,697
ligand	260
water	543
B-factors	
protein	33.9
ligand	32.5
water	32.7
R.m.s. deviations	
Bond lengths (Å)	0.003
Bond angles (°)	0.727

*Values in parentheses are for the highest-resolution shell.